

## **Supporting Information**

# **Coordinative integration of a metal-porphyrinic framework and TiO<sub>2</sub> nanoparticles for the formation of composite photocatalysts with enhanced visible-light-driven photocatalytic activities**

Yanming Zhao,<sup>ab</sup> Yuze Dong,<sup>a</sup> Futai Lu,<sup>a</sup> Chenggong Ju,<sup>a</sup> Lin Liu,<sup>a</sup> Jie Zhang,<sup>c</sup> Bao Zhang<sup>\*a</sup>  
and Yaqing Feng<sup>\*ab</sup>

<sup>a</sup>School of Chemical Engineering and Technology, Tianjin University, Tianjin, China 135,  
Yaguan Road, Jinnan district, Tianjin 300350, PR China.

<sup>b</sup>Tianjin Co-Innovation Center of Chemical Science and Engineering, Tianjin 300072, China.

<sup>c</sup>School of Science, Tianjin Chengjian University, Tianjin 300384, China.

\*Address correspondence to [baozhang@tju.edu.cn](mailto:baozhang@tju.edu.cn), [yqfeng@tju.edu.cn](mailto:yqfeng@tju.edu.cn).

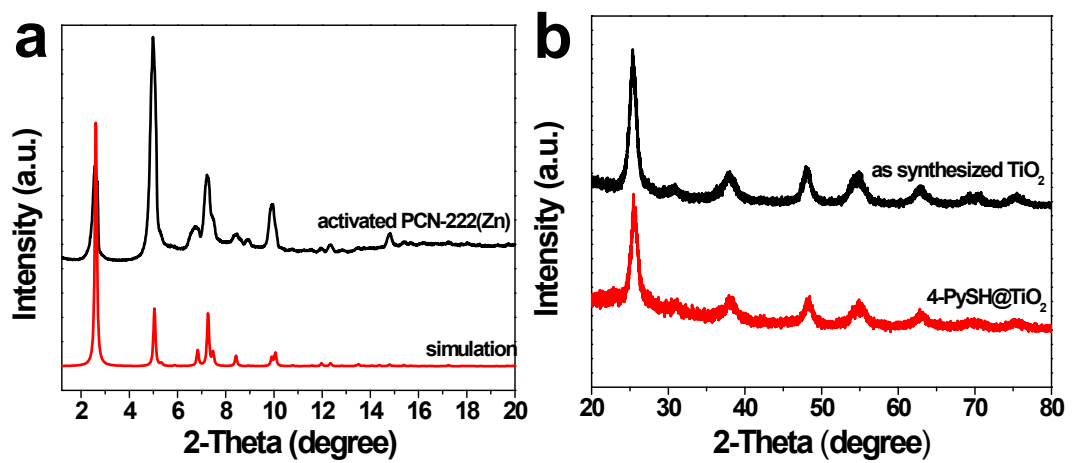


**Fig. S1** (a) XRD pattern of the as-synthesized PCN-222(Zn) and the simulated XRD pattern for the PCN-222(Zn) structure created from CIF in reference document. (b) XRD patterns of as-synthesized  $\text{TiO}_2$  and 4-PySH@ $\text{TiO}_2$ .

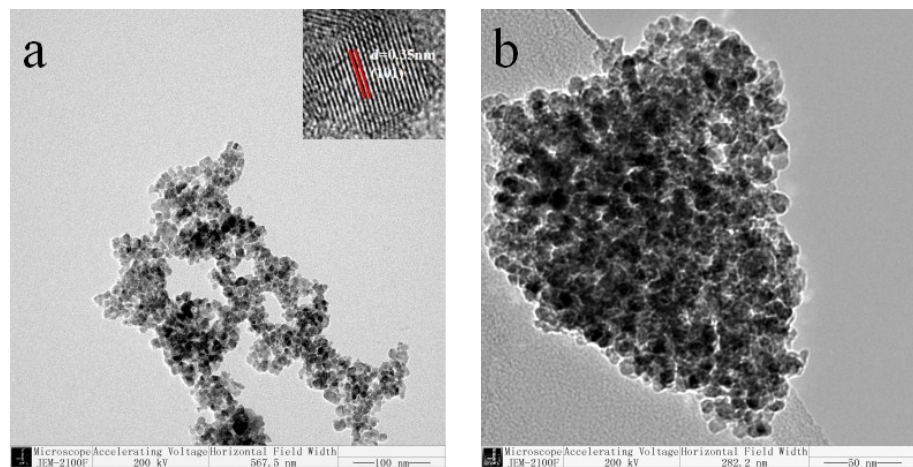


**Fig. S2** TEM images of (a) the pristine  $\text{TiO}_2$  and (b) the 4-PySH@ $\text{TiO}_2$  composite.

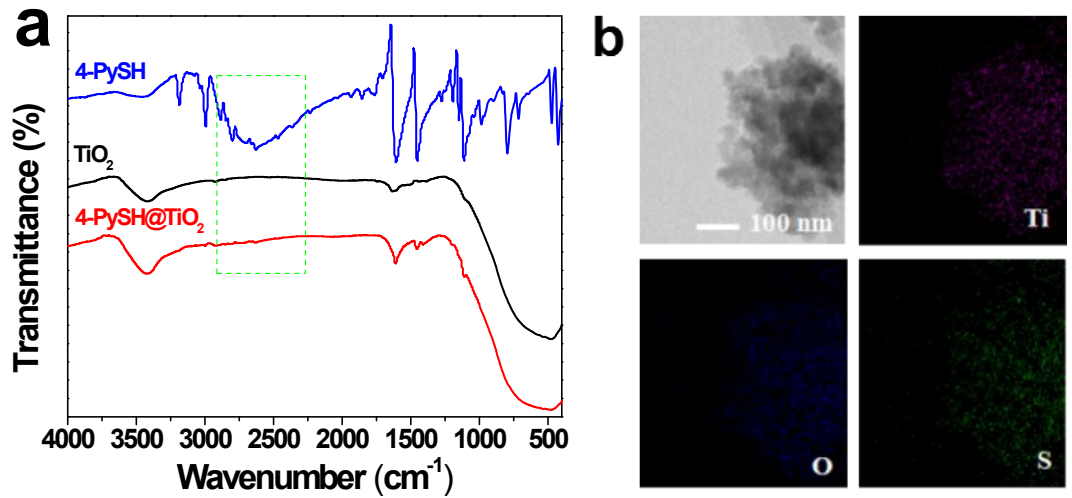


**Fig. S3** (a) FTIR spectra of 4-PySH, TiO<sub>2</sub> and 4-PySH@TiO<sub>2</sub>. (b) EDX elemental mappings of 4-PySH@TiO<sub>2</sub>.

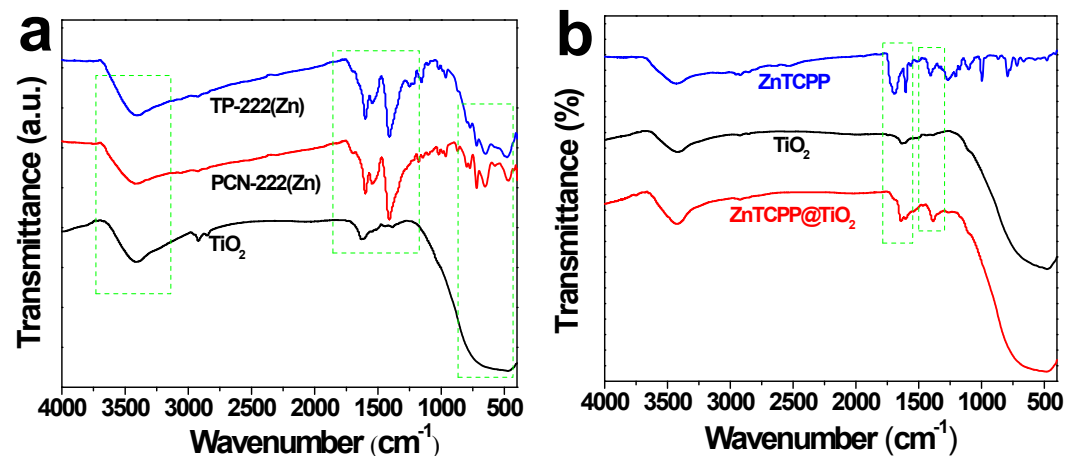


**Fig. S4** FTIR spectra of (a) TiO<sub>2</sub>, PCN-222(Zn) and TP-222(Zn) and (b) ZnTCPP, TiO<sub>2</sub> and ZnTCPP@TiO<sub>2</sub>.

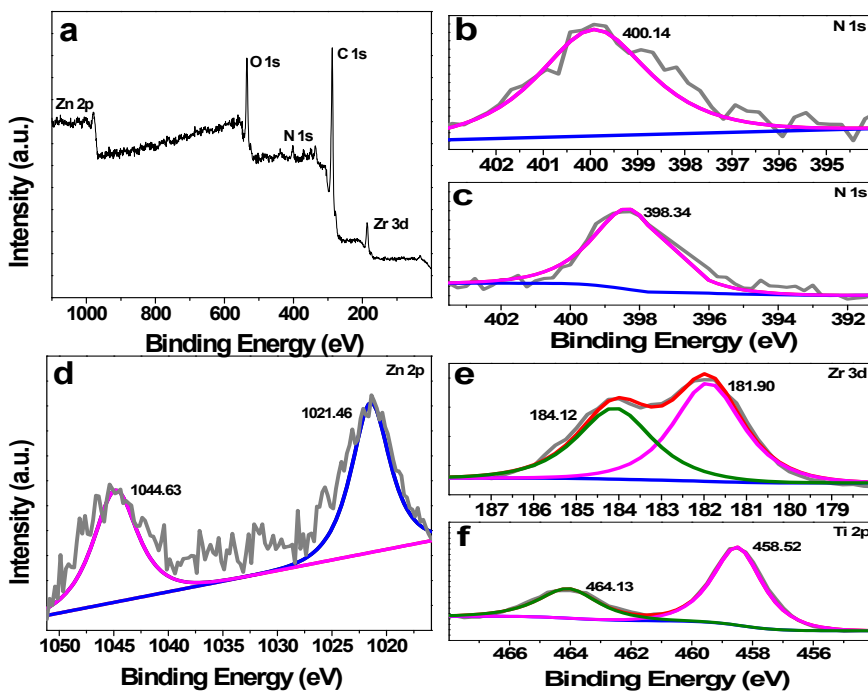


**Fig. S5** (a) XPS survey spectrum of PCN-222(Zn). (b) and (c) N 1s XPS spectrum of 4-PySH<sub>2</sub>@TiO<sub>2</sub> and PCN-222(Zn), respectively. (d) Zn 2p XPS spectrum of PCN-222(Zn). (e) and (f) Zr 3d and Ti 2p XPS spectrum of TP-222(Zn), respectively.

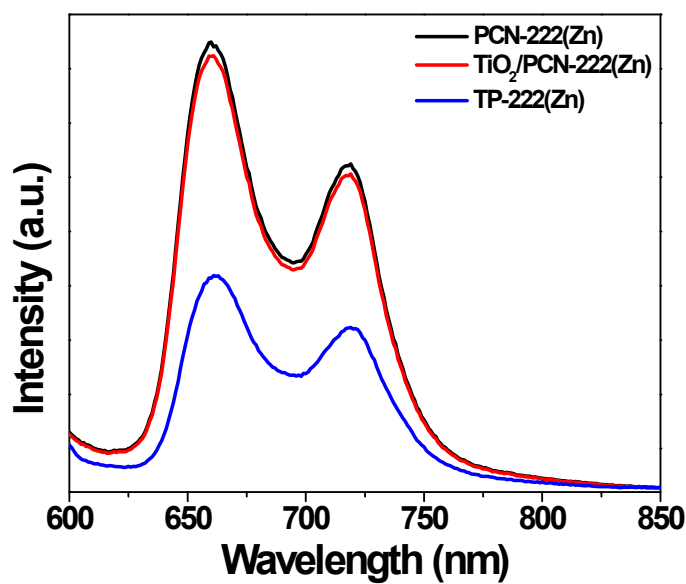


**Fig. S6** PL emission spectra (excited at 457 nm) of PCN-222(Zn), TiO<sub>2</sub>/PCN-222(Zn) and TP-222(Zn).

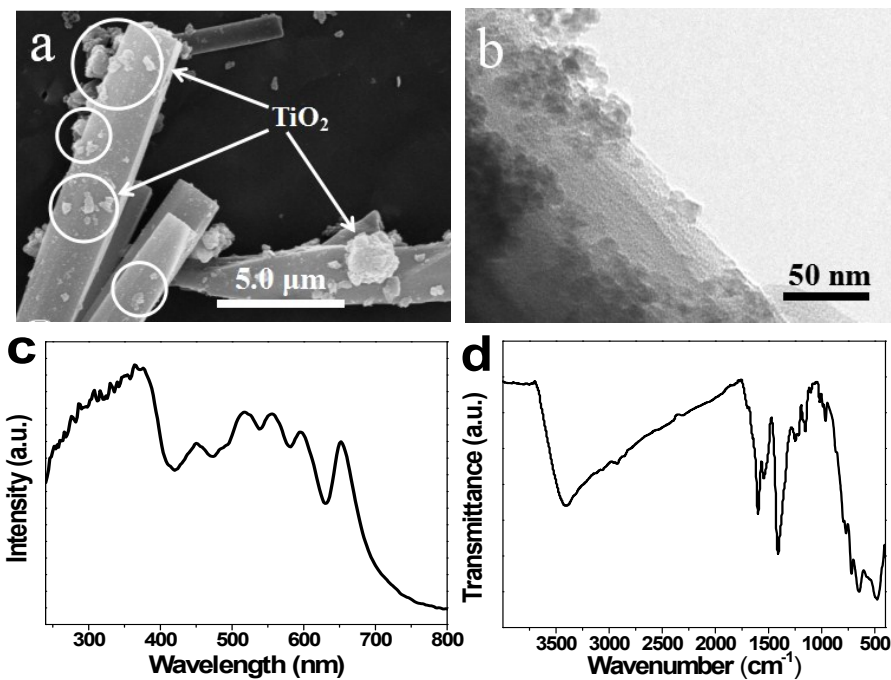


**Fig. S7** (a) SEM image, (b) TEM image, (c) UV-visible diffusive reflectance spectra and (d) FTIR spectra of the mixture of  $\text{TiO}_2$  and PCN-222(Zn) ( $\text{TiO}_2/\text{PCN-222}$ ).

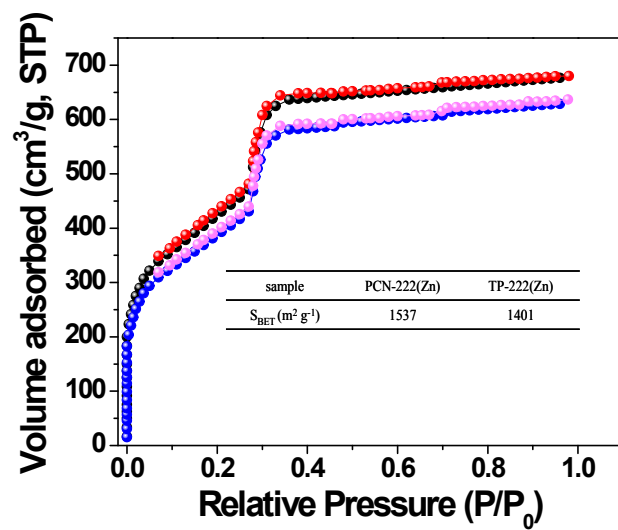


**Fig. S8**  $\text{N}_2$  adsorption-desorption isotherms measured for PCN-222(Zn) and TP-222(Zn) together with their specific surface area.

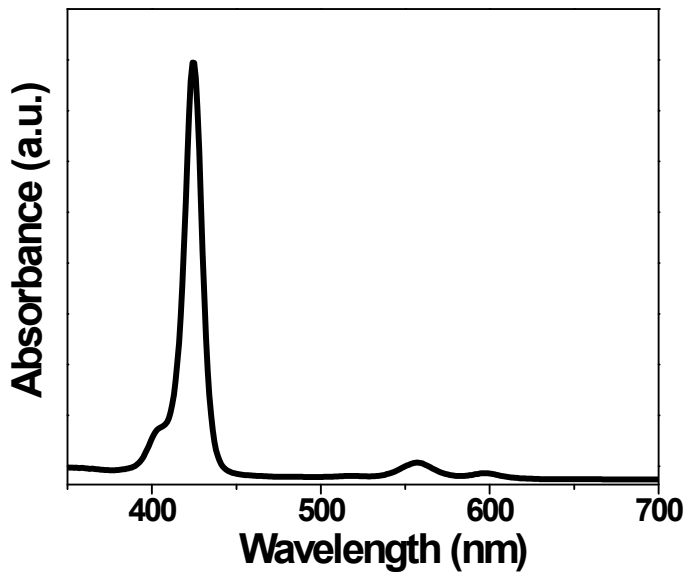


**Fig. S9** UV-visible absorption spectra of the porphyrinic ligand (ZnTCPP) of PCN-222(Zn) in DMF solution.

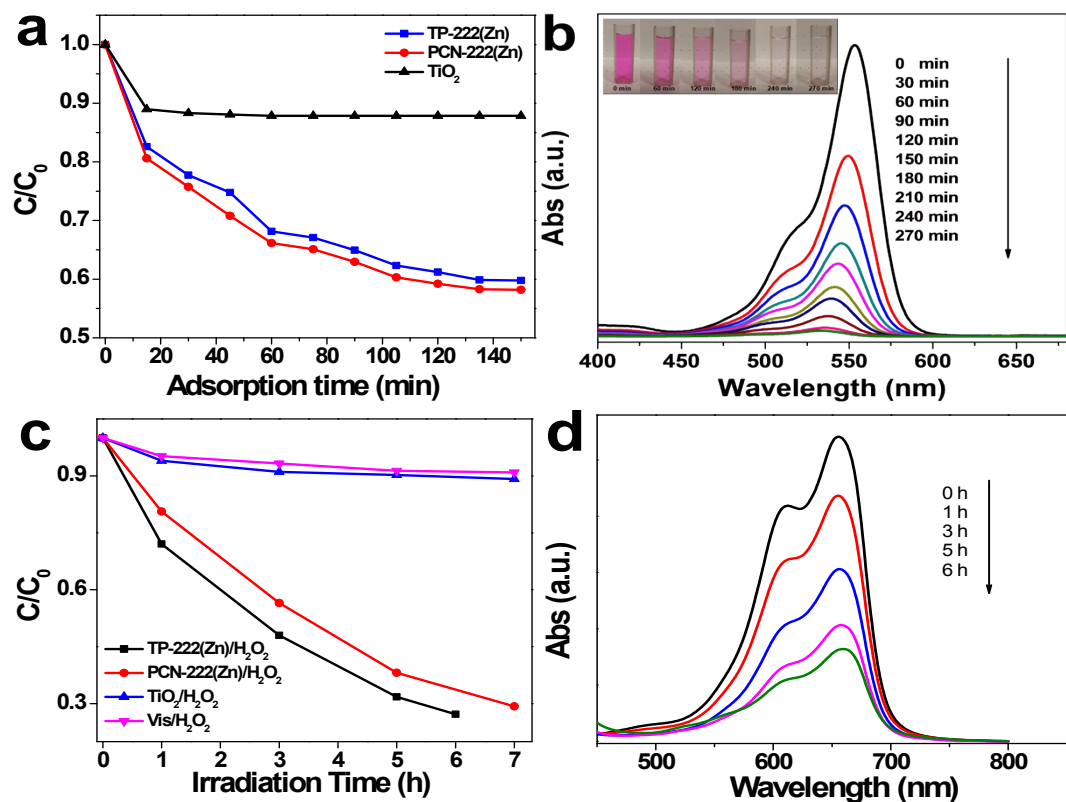


**Fig. S10** (a) Adsorption equilibrium plots of RhB solution over TP-222(Zn), PCN-222(Zn) and  $\text{TiO}_2$ . (c)  $C/C_0$  versus irradiation time curves for degrading MB. (b) and (d) Absorption spectra of RhB and MB solutions under different irradiation time by using TP-222(Zn), respectively. The inset shows the color changes of the RhB solutions corresponding to the six degradation times from 0 min to 270 min.

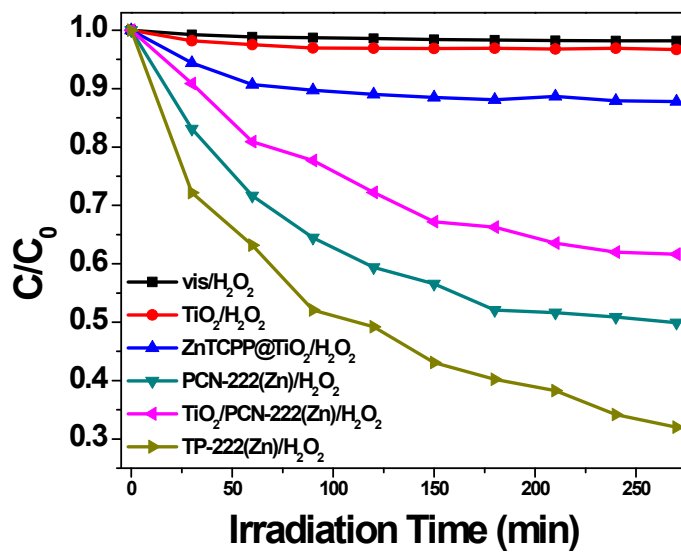


**Fig. S11** Degradation of 2,4-DNP in different photocatalytic systems under visible light irradiation. (Experimental conditions: samples, 2, 2.4 or 2.2 mg; 2,4-DNP, 50 ml/20 mg L<sup>-1</sup>; 30 wt% H<sub>2</sub>O<sub>2</sub>, 2 ml.)

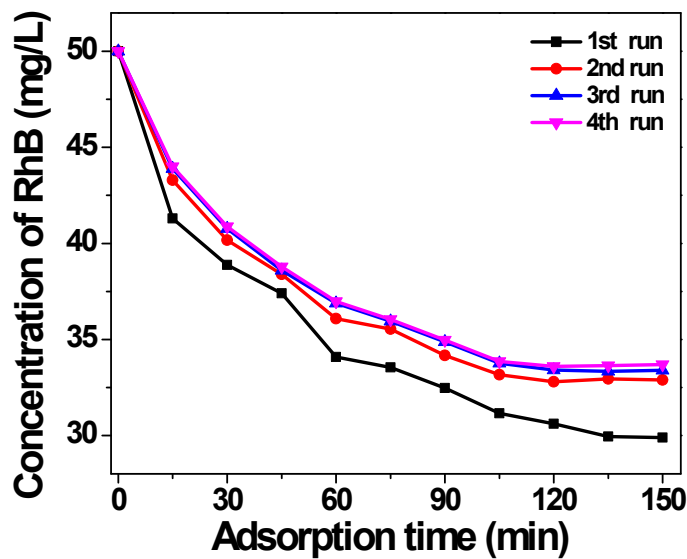


**Fig. S12** Adsorption equilibrium plots of RhB solutions over the TP-222(Zn) composite for four cycles.

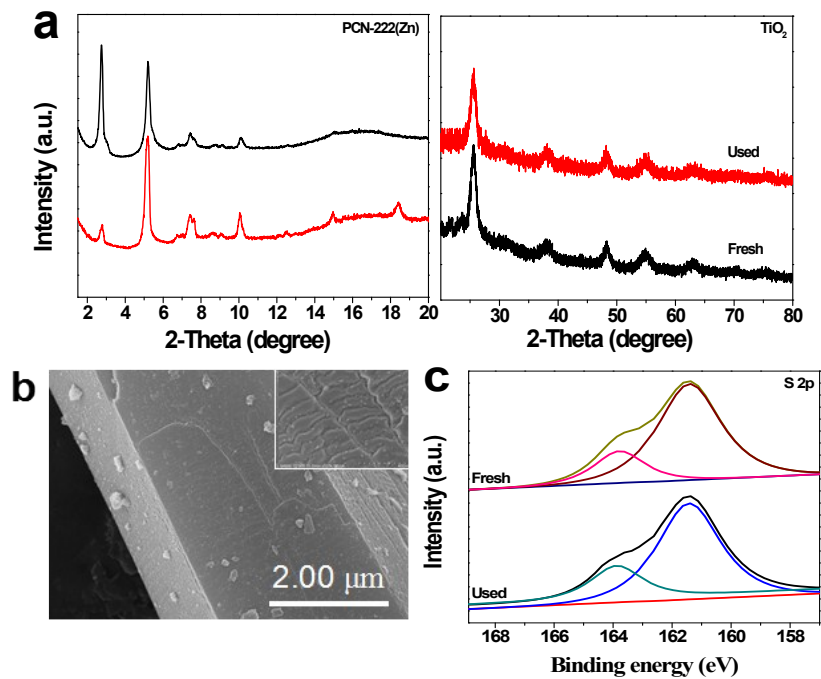


**Fig. S13** (a) XRD patterns of the TP-222(Zn) composite before and after four photocatalytic degradation cycles. (b) SEM images of the TP-222(Zn) composite after four photocatalytic degradation cycles under visible light irradiation. (c) Comparison of S 2p XPS spectrum of the TP-222(Zn) composite before and after four photocatalytic degradation cycles.

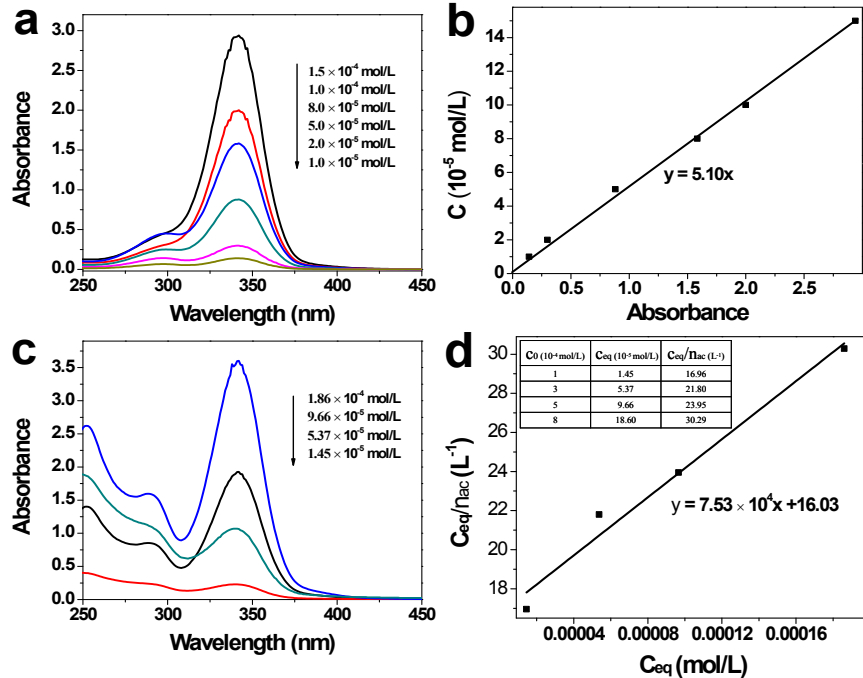


**Fig. S14** Binding constant measurements. (a) UV-Vis absorption spectra of 4-PySH with different concentrations. (b) The fitted plot of  $C$  (4-PySH in EtOH) *versus* absorbance together with the corresponding fitting function. (c) UV-Vis absorption spectra of 4-PySH after adsorbing on  $\text{TiO}_2$  NPs for 72 h. (d) The fitted plot of  $C_{\text{eq}}/n_{\text{ac}}$  *versus*  $C_{\text{eq}}$  together with the corresponding fitting function. The inset shows the values of  $C_0$ ,  $C_{\text{eq}}$  and  $C_{\text{eq}}/n_{\text{ac}}$ .

## Determining the binding constant of 4-PySH to TiO<sub>2</sub> surface.<sup>1</sup>

In these experiments, 50 mg TiO<sub>2</sub> NPs were immersed in four ethanol solutions of 4-PySH for 72 h (the concentrations are respectively  $1 \times 10^{-4}$ ,  $3 \times 10^{-4}$ ,  $5 \times 10^{-4}$  and  $8 \times 10^{-4}$  mol/L). TiO<sub>2</sub> NPs were subsequently removed by centrifugation and the supernatant was subjected to UV-Vis absorption spectroscopy analysis in order to determine the equilibrium concentration ( $C_{eq}$ ) of the 4-PySH ethanol solution. The adsorption capacity ( $n_{ac}$ ) of 4-PySH was calculated from the difference in the concentrations before and after equilibration with TiO<sub>2</sub> NPs, in which the concentrations were determined by the fitting function of C *versus* absorbance (as shown in Fig. S14b). Then, the data were plotted according to the Langmuir isotherm equation:

$$\frac{C_{eq}}{n_{ac}} = aC_{eq} + b$$

The binding constant ( $K$ , M<sup>-1</sup>) is calculated as  $K = a/b$  based on the fitted line in Fig. S14d.

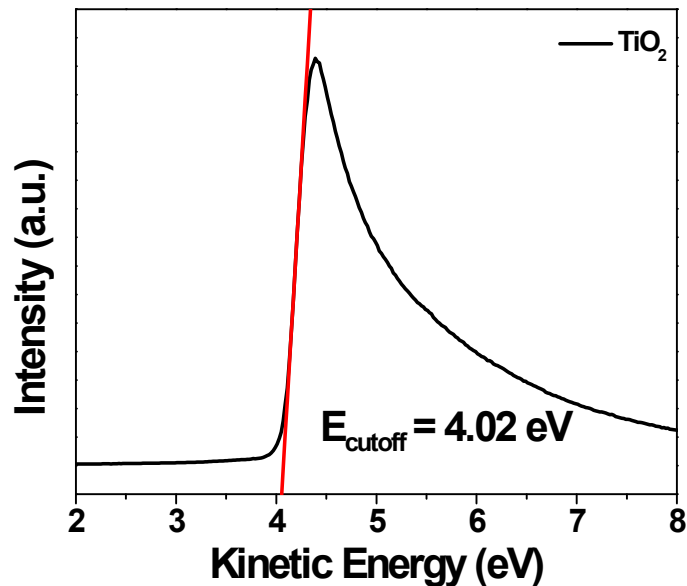


**Fig. S15** UPS spectra and  $E_{cutoff}$  of the pristine TiO<sub>2</sub>.

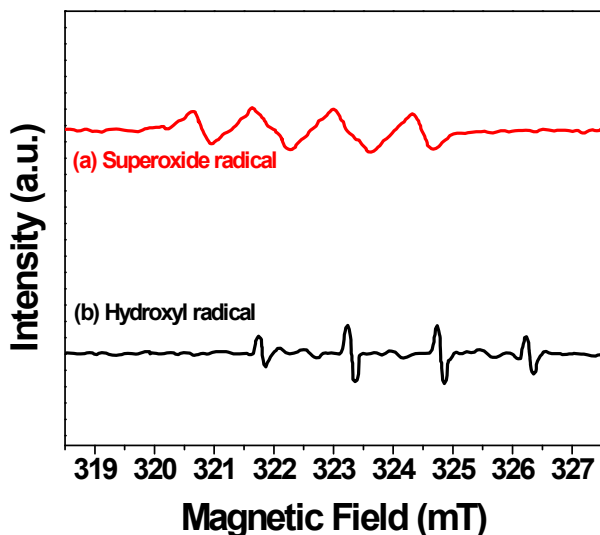


**Fig. S16** DMPO spin-trapping EPR spectra of the TP-222(Zn) without  $\text{H}_2\text{O}_2$  system in methanol dispersion for DMPO- $\cdot\text{O}_2^-$  (a) and the TP-222(Zn) with  $\text{H}_2\text{O}_2$  system in aqueous dispersion for DMPO- $\cdot\text{OH}$  (b).

**Table S1** The operating conditions used for ICP-MS measurements.

Nebulizer	Babington
Spray chamber	Quartz
Reaction gas flow rate	2 mL min <sup>-1</sup>
Carrier gas flow rate	1.15 L min <sup>-1</sup>
RF power	1500 W
Resolution (amu)	2 ~ 260
Integration time	1 s
Replicates	3
Detector mode	Auto
Analytical masses	Ti (47), Zr (92)

**Table S2** Loading amounts of  $\text{TiO}_2$  NPs in composite TP-222(Zn) determined by ICP-MS.

	Concentration ( $\mu\text{g L}^{-1}$ )		Loading amounts of $\text{TiO}_2$ NPs (wt.%)
	Ti	Zr	
Before photocatalysis	4.2	6.9	18.3
After photocatalysis	2.9	5.4	16.6
$\text{TiO}_2/\text{PCN-222(Zn)}$	0.9	4.5	7.6

The loading amounts of  $\text{TiO}_2$  NPs in the TP-222(Zn) composite or the mixture of  $\text{TiO}_2$  NPs and PCN-222(Zn) is calculated based on the detected concentrations of Ti and Zr and also based on the formula (C<sub>48</sub>H<sub>32</sub>ZnN<sub>4</sub>O<sub>16</sub>Zr<sub>3</sub>) of PCN-222(Zn) with the formula weight of 1259.84.<sup>[2]</sup>

**Table S3** Comparative study of the photocatalytic activity of the TP-222(Zn) composite with other materials including MOF materials and non-MOF materials in the complete photocatalytic degradation of RhB under visible light irradiation.

Catalysts	Volume of RhB solution (ml)	Conc. of RhB solution (mg L <sup>-1</sup> )	Conc. of catalyst (mg L <sup>-1</sup> )	Degradation time (min)	References
MIL-53(Fe)	25	10	400	70	[3]
g-C <sub>3</sub> N <sub>4</sub> /MIL-125(Ti)	100	50	400	60	[4]
Ag <sub>2</sub> CO <sub>3</sub> /UiO-66(Zr)	30	14.37	500	120	[5]
Fe <sub>2</sub> O <sub>3</sub> @SnO <sub>2</sub>	25	25	600	40	[6]
BiOCl	15	60	667	60	[7]
TiO <sub>2</sub> /CdS	70	15	1000	120	[8]
Ag <sub>3</sub> PO <sub>4</sub> /WS <sub>2</sub>	20	4.79	1000	10	[9]
3DOM g-C <sub>3</sub> N <sub>4</sub>	70	10	1000	40	[10]
Bi <sub>3</sub> NbO <sub>7</sub>	50	4.79	1000	50	[11]
Bi <sub>2</sub> WO <sub>6</sub>	100	10	500	50	[12]
Bi <sub>2</sub> S <sub>3</sub> /Bi <sub>2</sub> O <sub>2</sub> CO <sub>3</sub>	50	4.79	1000	30	[13]
TP-222(Zn)	50	50	48	270	This work

**Table S4** Dynamics analysis of emission decay of PCN-222(Zn) and TP-222(Zn).

	$\tau_1$ (ns) (Rel.%)	$\tau_2$ (ns) (Rel.%)	$\tau_{av}$ (ns)
PCN-222(Zn)	0.3 (68.6)	2.3 (31.4)	1.8
TP-222(Zn)	0.9 (59.8)	5.4 (40.2)	4.5

## Supplementary Reference

- 1 Y. Pellegrin, L. L. Pleux, E. Blart, A. Renaud, B. Chavillon, N. Szwarski, M. Boujtita, L. Cario, S. Jobic, D. Jacquemin and F. Odobel, *J. Photoch. Photobio.*, 2011, **219**, 235–242.
- 2 D.-W. Feng, Z.-Y. Gu, J.-R. Li, H.-L. Jiang, Z.-W. Wei and H.-C. Zhou, *Angew. Chem. Int. Ed.*, 2012, **51**, 10307–10310.
- 3 C.-H. Zhang, L.-H. Ai and J. Jiang, *J. Mater. Chem. A*, 2015, **3**, 3074–3081.
- 4 H. Wang, X.-Z. Yuan, Y. Wu, G.-M. Zeng, X.-H. Chen, L.-J. Leng and H. Li, *Appl. Catal., B*, 2015, **174–175**, 445–454.
- 5 Z. Sha, H. S. O. Chan and J.-S. Wu, *J. Hazard. Mater.*, 2015, **299**, 132–140.
- 6 N. Wang, Y.-C. Du, W.-J. Ma, P. Xu and X.-J. Han, *Appl. Catal., B*, 2017, **210**, 23–133.
- 7 W.-W. Liu, Y.-Y. Shang, A.-Q. Zhu, P.-F. Tan, Y. Liu, L.-L. Qiao, D.-W. Chu, X. Xiong and J. Pan, *J. Mater. Chem. A*, DOI: 10.1039/c7ta02724a
- 8 C. Xue, T. Wang, G.-D. Yang, B.-L. Yang and S.-J. Ding, *J. Mater. Chem. A*, 2014, **2**, 7674–7679.
- 9 H.-J. Yu, Y. Yu, J.-H. Liu, P.-Y. Ma, Y.-C. Wang, F. Zhang and Z.-Y. Fu, *J. Mater. Chem. A*, 2015, **3**, 19439–19444.
- 10 B. Lin, G.-D. Yang, B.-L. Yang and Y.-X. Zhao, *Appl. Catal., B*, 2016, **198**, 276–285.
- 11 Q.-Q. Wang, L.-P. Yuan, M. Dun, X.-M. Yang, H. Chen, J.-L. Li and J.-C. Hu, *Appl. Catal., B*, 2016, **196**, 127–134.
- 12 C.-M. Li, G. Chen, J.-X. Sun, H.-J. Dong, Y. Wang, C.-D. Lv, *Appl. Catal., B*, 2014, **160–161**, 383–389.
- 13 N. Liang, J.-T. Zai, M. Xu, Q. Zhu, X. Wei and X.-F. Qian, *J. Mater. Chem. A*, 2014, **2**, 4208–4216.